

# Enhancing hydrodynamics simulations in Distillation Columns Using Smoothed Particle Hydrodynamics (SPH)

Rodolfo Murrieta-Dueñas<sup>a</sup>, Jazmín Cortez-González<sup>a</sup>, Roberto Gutiérrez-Guerra<sup>b</sup>, Juan Gabriel Segovia Hernández<sup>c</sup>, Carlos E. Alvarado-Rodríguez<sup>c,d</sup>

<sup>a</sup> Tecnológico Nacional de México / Campus Irapuato, Department of Chemical Engineering, Irapuato, Guanajuato, México

<sup>b</sup> Universidad Tecnológica de Leon, Sustainability for Development Department, León, Guanajuato, México

<sup>c</sup> Universidad de Guanajuato, Department of Chemical Engineering, Guanajuato, Guanajuato, México.

<sup>d</sup> Secretaría de Ciencias, Humanidades, Tecnología e Innovación, Ciudad de México, México

\* Corresponding Author: [rodolfo.md@irapuato.tecnm.mx](mailto:rodolfo.md@irapuato.tecnm.mx)

## ABSTRACT

This study presents a numerical simulation of the liquid-vapor (L-V) equilibrium stage in a sieve plate distillation column using the Smoothed Particle Hydrodynamics (SPH) method. To simulate the equilibrium stage, periodic temperature boundary conditions were applied. The column design was carried out in Aspen One, considering an equimolar benzene-toluene mixture and an operating pressure ensuring a condenser cooling water temperature of 120°F. The Chao-Seader thermodynamic model was employed for property calculations. Key outputs included liquid and vapor velocities per stage, mixture viscosity and density, operating pressure, and column diameter. The geometry of the distillation column stage and sieve plate was developed using SolidWorks, and Computational Fluid Dynamics (CFD) simulations were performed using the DualSPHysics code. The results demonstrate the influence of sieve plate design on velocity and temperature distributions within the stage, providing insights for enhancing stage design and operational efficiency.

**Keywords:** CFD, Simulation of distillation, hydrodynamics, SPH, Sieve tray

## 1. INTRODUCTION

Distillation remains the most widely utilized unit operation in Chemical Engineering due to its exceptional capability for product purification. However, conventional distillation processes are often associated with significant inefficiencies, driving the pursuit of alternative strategies to improve thermodynamic efficiency in equipment design and operation. While many of these alternatives have been evaluated using MESH equations and sequential simulators, less attention has been given to their modeling using Computational Fluid Dynamics (CFD), primarily due to its inherent complexity.

CFD employs either Eulerian or Lagrangian approaches. Eulerian methods rely on mesh-based discretization of the medium, producing spatially averaged results at the interfaces between fluids. Examples include the finite volume and finite element methods, with the former being widely adopted for simulating hydrodynamics, mass transfer, and momentum within distilla-

tion columns (Haghshenas et al., 2007; Lavasani et al., 2018; Zhao, 2019; Ke, 2022). However, Eulerian methods face limitations, including challenges in interface modeling, achieving convergence, and selecting appropriate turbulence models to accurately simulate turbulent flows.

In contrast, Lagrangian methods provide detailed insights into interfacial phenomena by discretizing the continuous medium into mesh-free points. This approach enables precise evaluation of flow, concentration, and temperature distributions within a system. Smoothed Particle Hydrodynamics (SPH) is a Lagrangian method particularly suited for modeling discontinuous media and complex geometries. It replaces the need for mesh generation by representing the medium with particles, making it applicable to a wide range of scenarios, including microbial growth (Martínez-Herrera et al., 2022), sea wave dynamics (Altomare et al., 2023), and stellar phenomena (Reinoso et al., 2022), demonstrating its flexibility and robustness.

Building on these advantages, this study presents a numerical simulation of a liquid-vapor (L-V) thermal equilibrium stage within a tray distillation column using the SPH method. The study focuses on Sieve trays, incorporating periodic temperature conditions to facilitate the simulation of the equilibrium stage.

## 2. METHODOLOGY

In this work a methodology for the simulation of the hydrodynamics and thermal equilibrium of tray distillation columns is proposed. This methodology consists of 3 stages: rigorous design of the distillation column in Aspen Plus, 3D design of the column - sieve trays and hydrodynamic analysis of the columns using the SPH method.

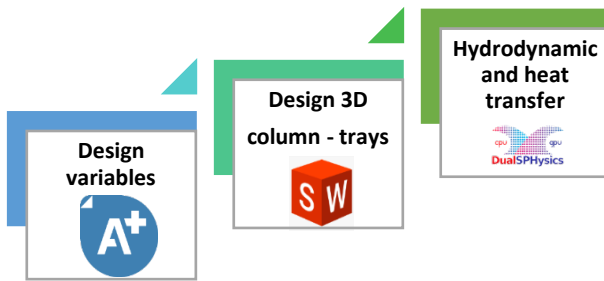


**Figure 1.** Methodology for the numerical simulation of the hydrodynamics and equilibrium of distillation columns.

### 2.1. Rigorous design of the distillation column

The column's sizing was conducted using Aspen One, considering an equimolar mixture of Benzene-Toluene and an operational pressure guaranteeing a condenser cooling water temperature of 120°F. The thermodynamic model applied was Chao-Seader, and sieve trays were employed. The column featured ten stages, with stage 5 designated for feeding, and both components assumed a 98% purification and recovery rate. This information yielded crucial data, including liquid and vapor velocities per stage, mixture viscosity and density, operating pressure, and column diameter. Three-dimensional CAD files of the distillation column and the sieve tray were developed using SolidWorks. Subsequently, these files were imported into DualSPHysics (Domínguez et. al., 2022) for CFD numerical simulation to ascertain flow and temperature profiles at an equilibrium stage. Stage 7 was selected for analysis, given their position below the feed stage.

The design of the distillation column was performed by rigorous methods, solving the MESH equations. **M** represents the total mass balance and the mass balance per component. **E** represents the equilibrium ratios present in the distillation process. **S** represents the sum of the mole fractions of the components of the mixture. **H** represents the total heat balance of the dis-

tillation column. This model is represented by equations 1 to 4.

Mass balance:

$$\frac{dM_j}{dt} = L_{j-1} + V_{j+1} + F_j^L + F_j^V - (L_j + U_j) - (V_j + W_j) \quad (1)$$

Equilibrium relationships:

$$Y_{i,j} = K_{i,j} X_{i,j} \quad (2)$$

Summation constraints:

$$\sum_{i=1}^{NC} K_{i,j} X_{i,j} - 1.0 = 0 \quad (3)$$

Energy balance:

$$\frac{d(M_j \bar{U}_{i,j})}{dt} = L_{j-1} \bar{h}_{j-1} + V_{j+1} \bar{H}_{j+1} + F_j^L \bar{h}_j^L + F_j^V \bar{H}_j^V - (L_j + U_j) \bar{h}_j - (V_j + W_j) \bar{H}_j + Q_j \quad (4)$$

### 2.2. Column and sieve tray sizing

The 3D design of the column and trays was carried out in SolidWorks. The design parameters used were: column diameter, effective and downspout areas, obtained in Aspen Plus. The distance between trays was proposed to be 0.15m. Stainless steel 316L was chosen as construction material. Figure 2 shows, the 3D design of the tray, the stage and the initial conditions.

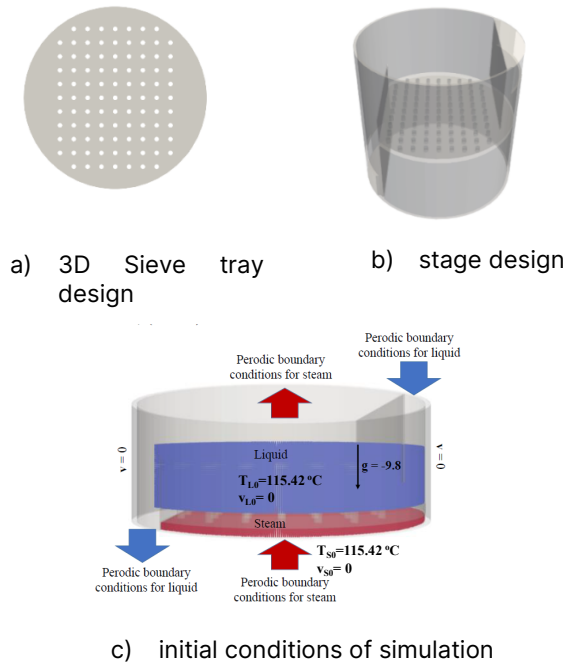


**Figure 2.** Sieve tray design to simulation.

**Table 1.** Results of the rigorous simulation of the distillation column in Aspen Plus.

Parameter	Líquid	Vapor
<b>Density (kg/m<sup>3</sup>)</b>	783.8023	4.0206
<b>Viscosity (Ns/m<sup>2</sup>)</b>	2.5x10 <sup>-4</sup>	9.5x10 <sup>-6</sup>
<b>Temperature (°C)</b>	105.99	115.42
<b>Mass fraction</b>	0.5886	0.5405
<b>Velocity (m/s)</b>	0.0261	0.0214
<b>Coefficient of thermal diffusivity (m<sup>2</sup>/s)</b>	7.9247x10 <sup>-8</sup>	
<b>Surface tension</b>	0.018 N/m	0.018 N/m

### 2.3. Hydrodynamics and heat transfer

Smoothed Particle Hydrodynamics (SPH) is a Lagrangian, meshless method with applications in the field of Computational Fluid Dynamics. Originally invented for astrophysics in the 1970s (Monagan J, 1992) it has been applied in many different fields, including fluid dynamics (Alvarado-Rodríguez C.E. et al., 2019). The method uses points named particles to represent the continuum and these particles move according to the governing equations in the fluid dynamic. When simulating free-surface flows, no special surface treatment is necessary due to the Lagrangian nature of SPH, making this technique ideal for studying violent free-surface motion.

For the numerical simulation the conservation equations of mass (Eq. 5), momentum (Eq. 6) and energy (Eq. 7) in Lagrangian formalism are considered.

$$\frac{d\rho}{dt} = -\rho \nabla \cdot \mathbf{v} \quad (5)$$

$$\frac{d\mathbf{v}}{dt} = \frac{-1}{\rho} \nabla P + \frac{\mu}{\rho} \nabla^2 \mathbf{v} + \mathbf{g} + \mathbf{F}^B \quad (6)$$

$$\frac{dT}{dt} = \frac{1}{\rho C_p} \nabla \cdot (k \nabla T) \quad (7)$$

where  $\rho$  is the density,  $t$  is the time,  $\mathbf{v}$  is the velocity vector,  $P$  is the pressure,  $\mu$  is the viscosity,  $\mathbf{g}$  is the gravitational acceleration vector,  $T$  is the temperature,  $C_p$  is the heat capacity and  $k$  is the thermal conductivity coefficient.

The motion of the fluid due to the change in temperature is provided by Boussinesq approximation (Eq. 8):

$$\mathbf{F}^B = -\mathbf{g}\beta(T - T_r) \quad (8)$$

where  $\beta$  is the thermal coefficient of volumetric expansion, and  $T_r$  is the reference temperature of the fluid.

The momentum, continuity and energy equations can be discretized using the SPH formalism and gives:

$$\frac{d\rho_a}{dt} = -\rho_a \sum_b^n m_b \frac{\mathbf{v}_b}{\rho_b} \cdot \nabla W_{ab} \quad (9)$$

$$\begin{aligned} \frac{d\mathbf{v}_a}{dt} = & -\sum_b^n m_b \left( \frac{P_b}{\rho_b^2} + \frac{P_a}{\rho_a^2} \right) \nabla_a W_{ab} \\ & + \sum_b^n m_b \frac{4v r_{ab} \cdot \nabla W_{ab}}{(\rho_a + \rho_b)(r_{ab}^2 + \varepsilon^2)} \mathbf{v}_{ab} \\ & + \mathbf{F}^B \end{aligned} \quad (10)$$

$$\frac{dT}{dt} = \frac{1}{C_p} \sum_b^n \frac{m_b}{\rho_a \rho_b} \frac{(k_a + k_b)r_{ab} \cdot \nabla_a W_{ab}}{r_{ab}^2 + \varepsilon^2} (T_a - T_b) \quad (11)$$

Equations (Eq. 9)-(Eq. 11) are coupled by the Tait state equation (Eq. 12)

$$P = B \left[ \left( \frac{\rho}{\tilde{\rho}} \right)^\gamma - 1 \right] \quad (12)$$

where  $P$  is the pressure,  $\tilde{\rho}$  is the reference density,  $B = c^2 \rho / \gamma$ ,  $\gamma = 7 = 7$  for liquids and  $\gamma = 1.4$  for gases.

Different approaches and methods have been proposed to simulate multiphase flows (Tartakovsky & Meakin, 2006; Monaghan & Kocharyan, 1995; Sigalotti et al., 2014). In this work several new approaches are added to the standard formalism. These features permit to properly simulate multiphase flows, where the main contribution lies in the improved management to interphase with highly nonlinear deformations.

The instability and artificial surface tension produced in a multiphase flow using the standard SPH has been reported by (Colagrossi & Landrini, 2003, and Gómez Gesteira et al, 2010). For this work we have replaced the Eq. (10) used in the standard SPH formulation by the Eq. (13) which to permit that higher density ratios in simulations avoiding the artificial surface tension (Colagrossi & Landrini, 2003). The method is rather robust, even for large free-surface fragmentation and folding, efficient and relatively easy-to-code and results stable and capable to easily treat a variety of density ratios.

$$\begin{aligned} \frac{d\mathbf{v}_a}{dt} = & -\sum_b^n m_b \left( \frac{P_b + P_a}{\rho_a \rho_b} \right) \nabla_a W_{ab} \\ & + \sum_b^n m_b \frac{4v r_{ab} \cdot \nabla W_{ab}}{(\rho_a + \rho_b)(r_{ab}^2 + \varepsilon^2)} \mathbf{v}_{ab} \\ & + \mathbf{F}^B \end{aligned} \quad (13)$$

Higher density ratios can be simulated with the use of this expression avoiding the artificial surface tension.

According to (Colagrossi & Landrini, 2003) the pressure of each phase is calculated using the equation of state (14), which is calculated using appropriate parameters according to each phase reference density. So, the equation of state (14) is calculated for each phase using:

$$P_\alpha = B_\alpha \left[ \left( \frac{\rho}{\tilde{\rho}_\alpha} \right)^{\gamma_\alpha} - 1 \right] \quad (14)$$

where the subscripts  $\alpha$  denote the phase

The constant  $B_\alpha$  is chosen from the liquid phase to permit a small compressibility of the higher density fluid, that is  $v_{max\alpha} = c_\alpha \ll 1$ , where  $v_{max\alpha}$  is the maximum velocity of the fluid with higher density expected in the considered problem. Then  $B_\alpha$  must be matched to the liquid and gas phases in the equation of state for the fluid with lower density to create a stable pressure at the interphase. This formulation allows the simulation of high-density ratios (e.g. 1:1000, which is like the air-water ratio).

This method was implemented for the numerical analysis of the distillation columns under the following considerations: periodic conditions were used to perform the hydrodynamic and equilibrium analysis. The initial properties of the fluids are shown in Table 1. In all cases, no-slip boundary conditions were considered in the interaction between fluid and boundary particles using the dynamic particle method.

### 3. DISCUSSION OF RESULTS

From the results obtained using the SPH method in numerical simulations, it is possible to analyze the velocity profile and the temperature profile inside the stage. In addition, it is possible to approximate the time it requires for the stage to reach equilibrium under the initial conditions established.

The simulation was performed with a total of 7,261,750 particles of which 1,386,940 are bound, 4,230,940 are liquid and 1,643,870 are vapor. 60 seconds of real time were simulated. The simulation was completed in a total of 17.5h on the GPU NVIDIA GeForce 3060 of ITESI.

In Figure 3 is shown the evolution of velocity field obtained in the simulation. A higher velocity is obtained in the area where the fluid enters from the downspout, the velocity distribution is not completely homogeneous, however, there are not dominant streamlines in the stage, meaning a good distribution of the flow in the stage.

In Figure 4 the evolution of the temperature in the stage is shown, which due to the good flow get the equilibrium temperature in the simulated time. It is observed that in the downcomer section the fluid velocity is the highest and that the velocity distribution is uniform throughout the tray.

In Figure 5 is shown the distribution of the temperature from a top perspective at 22.5 seconds. The distribution of the temperature is almost homogeneous at this time. The liquid temperature and vapor temperature are very nearly at equilibrium. In addition, vapor accumulation zones can be observed which show very high temperatures and therefore no interaction between liquid and vapor.

In Figure 6 is shown a Reynolds map from a top perspective calculated from the average velocity shown in the Figure 3. This figure shows that the highest Reynolds values occur in the holes of the deck area and are consistent with the thermal behavior of Figure 5. This shows that the greater the interaction of the liquid with the vapor, the greater the heat transfer.

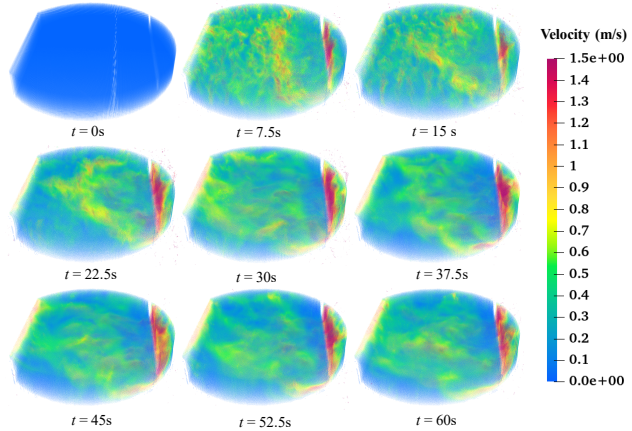


**Figure 3.** 3D perspective of the velocity field evolution in the stage.

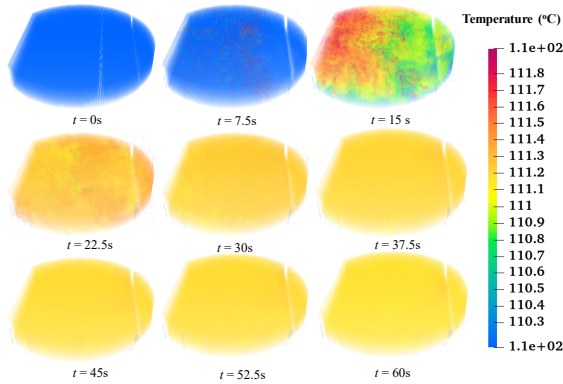


**Figure 4.** 3D perspective of the temperature field evolution in the stage.

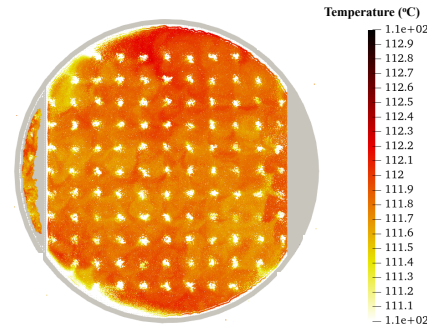


**Figure 5.** Top perspective of the temperature distribution.

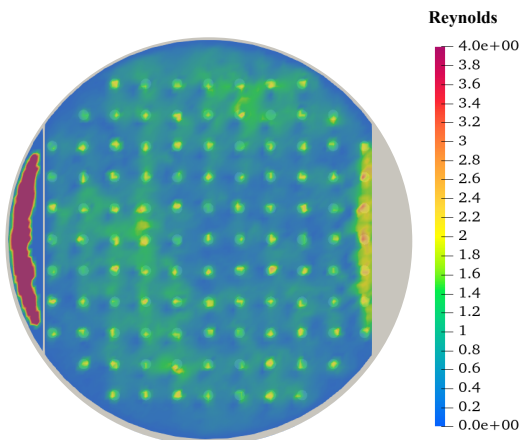


**Figure 6.** Top perspective of the Reynolds map calculated from the average velocity shown in Figure 3.

## 4. CONCLUSIONS

This study presents the CFD numerical simulation of a stage within a distillation column. The column and tray geometries were designed in SolidWorks and subsequently exported to DualSPHysics to carry out simulations based on parameters obtained from rigorous simulations in Aspen Plus. The numerical simulations provide detailed insights into the flow and heat transfer within the stage, accounting for the interaction between the vapor and liquid phases and their respective temperature variations. This data enables the development of a novel methodology for calculating the global heat transfer coefficient in the stage, which can be leveraged to enhance tray design and facilitate comparative analyses of different tray types. In conclusion, the results highlight the effectiveness of applying initial and boundary conditions to simulate thermal equilibrium in distillation columns. Additionally, the SPH method proves to be a powerful and flexible tool for numerical simulations of fluid dynamics and thermal equilibrium, offering valuable contributions to the design and optimization of distillation equipment.

## ACKNOWLEDGEMENTS

We are in agreement with the National Technological Institute of Mexico for the support provided for this research.

## REFERENCES

1. Altomare C, Scandura P, Cáceres I, van der A D, Viccione G. 2023. Large-scale wave breaking over a barred beach: SPH numerical simulation and comparison with experiments. *Coastal Engineering*, 185, 104362. doi:10.1016/j.coastaleng.2023.104362
2. Alvarado-Rodríguez, C. E., Klapp, J., Domínguez, J. M., Uribe-Ramírez, A. R., Ramírez-Minguela, J. J., & Gómez-Gesteira, M. (2019, March). Multiphase Flows Simulation with the Smoothed Particle Hydrodynamics Method. In *International Conference on Supercomputing in Mexico* (pp. 282-301). Springer, Cham.
3. Domínguez JM, Fourtakas G, Altomare C, Canelas RB, Tafuni A, García-Feal O, Martínez-Estevez I, Mokos A, Vacondio R, Crespo AJC, Rogers BD, Stansby PK, Gómez-Gesteira M. (2021), DualSPHysics: from fluid dynamics to multiphysics problems. *Computational Particle Mechanics*.
4. Haghshenas Fard, M., Zivdar, M., Rahimi, R., Nasr Esfahani, M., Afacan, A., Nandakumar, K., & Chuang, K. T. (2007). CFD simulation of mass transfer efficiency and pressure drop in a structured packed distillation column. *Chemical Engineering & Technology: Industrial Chemistry-Plant Equipment-Process Engineering-Biotechnology*, 30(7), 854-861. Martínez-
5. Herrera, G., Cortez-González, J., Murrieta-Dueñas, R., Uribe-Ramírez, A. R., Pérez-Segura, T., & Alvarado-Rodríguez, C. E. (2022). Smoothed particles hydrodynamics simulations of microbial kinetic in a stirred bioreactor with proximity impellers. *Computational Particle Mechanics*, 1-13.
6. Ke, T. (2022). CFD simulation of sieve tray hydrodynamics using openfoam.
7. Lavasani, M. S., Rahimi, R., & Zivdar, M. (2018). Hydrodynamic study of different configurations of sieve trays for a dividing wall column by using experimental and CFD methods. *Chemical Engineering and Processing-Process Intensification*, 129, 162-170.
8. Reinoso, B., Leigh, N. W., Barrera-Retamal, C. M., Schleicher, D., Klessen, R. S., & Stutz, A. M. (2022). The mean free path approximation and stellar collisions in star clusters: numerical exploration of the analytic rates and the role of perturbations on binary star mergers. *Monthly Notices of the Royal Astronomical Society*, 509(3), 3724-3736.
9. Zhao, H., Li, Q., Yu, G., Dai, C., & Lei, Z. (2019). Performance analysis and quantitative design of a flow-guiding sieve tray by computational fluid dynamics. *AIChE Journal*, 65(5), e16563
10. Martínez-Herrera, G., Cortez-González, J., Murrieta-Dueñas, R., Uribe-Ramírez, A. R., Pérez-Segura, T., & Alvarado-Rodríguez, C. E. (2022). Smoothed particles hydrodynamics simulations of microbial kinetic in a stirred bioreactor with proximity impellers. *Computational Particle Mechanics*, 9(5), 1017-1029.
11. Tartakovsky, A., Meakin, P.: Pore scale modeling of immiscible and miscible fluid flows using smoothed particle hydrodynamics. *Adv. Water Resour.* 29,

1464–1478 (2006).

- 12. Monaghan, J.J., Kocharyan, A.: SPH simulation of multi-phase flow. *Comput. Phys. Commun.* 87, 225–235 (1995).
- 13. Sigalotti, L.D.G., Troconis, J., Sira, E., Peña-Polo, F., Klapp, J.: Diffuse-interface modeling
- 14. of liquid-vapor coexistence in equilibrium drops using smoothed particle hydrodynamics.
- 15. *Phys. Rev. E* 90, 013021 (2014).
- 16. Colagrossi, A., Landrini, M.: Numerical simulation of interfacial flows by smoothed particle hydrodynamics. *J. Comput. Phys.* 191, 448–475 (2003)
- 17. Gómez-Gesteira, M., Rogers, B.D., Dalrymple, R.A., Crespo, A.J.C.: State of the art of classical SPH for free-surface flows. *J. Hydraul. Res.* 48, 6–27 (2010).

© 2025 by the authors. Licensed to PSEcommunity.org and PSE Press. This is an open access article under the creative commons CC-BY-SA licensing terms. Credit must be given to creator and adaptations must be shared under the same terms. See <https://creativecommons.org/licenses/by-sa/4.0/>

